Chem

CellPress

Article

Rational Molecular Design for Achieving Persistent and Efficient Pure Organic Room-Temperature Phosphorescence

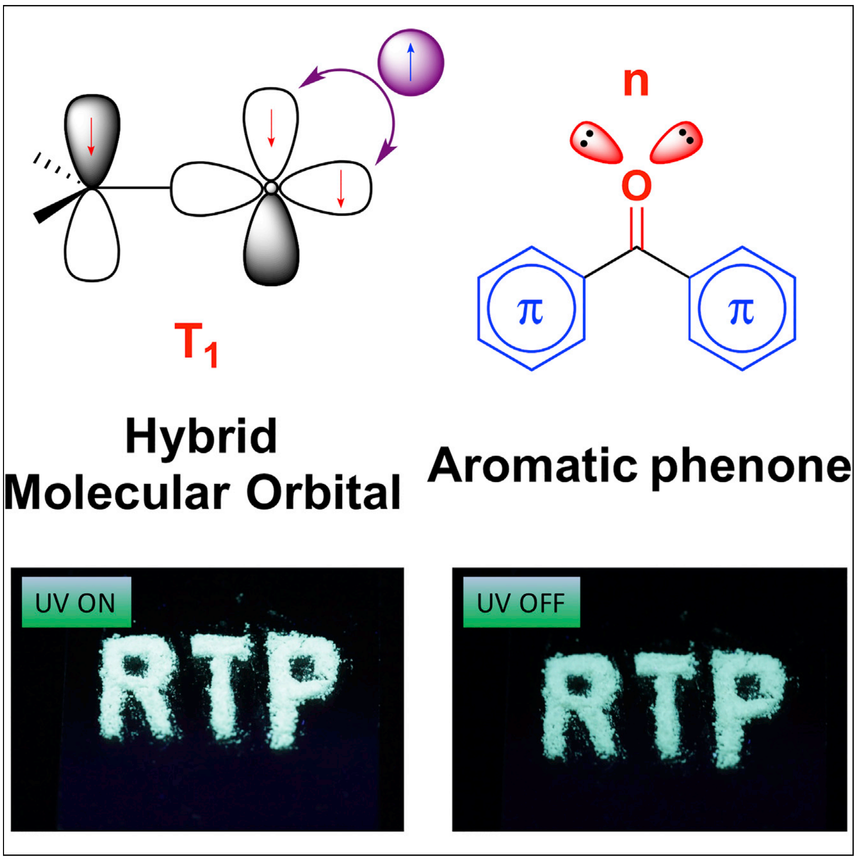

Theoretical investigations reveal the underlying relationship between the proportion of n and π orbitals and the rate of intersystem crossing and phosphorescence decay. Accordingly, Tang and colleagues have designed and synthesized a series of full-color pure organic phosphors with an efficiency of up to 36.0% and a long lifetime of 0.23 s under ambient conditions.

Weijun Zhao, Zikai He, Jacky W.Y. Lam, ..., Gongxun Bai, Jianhua Hao, Ben Zhong Tang

qpeng@iccas.ac.cn (Q.P.)
tangbenz@ust.hk (B.Z.T.)

HIGHLIGHTS

Balanced performance for pure organic room-temperature phosphorescence

Conflict of efficiency and lifetime for room-temperature phosphorescence

Molecular-orbital feature for persistent and efficient room-temperature phosphor

Zhao et al., Chem 1, 592–602
October 13, 2016
http://dx.doi.org/10.1016/j.chempr.2016.08.010

Chem

CellPress

Article

Rational Molecular Design for Achieving Persistent and Efficient Pure Organic Room-Temperature Phosphorescence

Weijun Zhao,[1,7] Zikai He,[1,7] Jacky W.Y. Lam,[1] Qian Peng,[2,*] Huili Ma,[3] Zhigang Shuai,[3] Gongxun Bai,[4] Jianhua Hao,[4] and Ben Zhong Tang[1,5,6,8,*]

SUMMARY

Manipulation of the emission properties of pure organic room-temperature phosphors through molecular design is attractive but challenging. Tremendous efforts have been made to modulate their aggregation behaviors to suppress nonradiative decay in order to achieve efficient light emission and long lifetimes. However, success has been limited. To attain such a goal, here we present a rational design principle based on intrinsic molecular-structure engineering. Comprehensive investigations on the molecular orbitals revealed that an excited state with hybrid (n,π*) and (π,π*) configurations in appreciable proportion is desired. Tailoring the aromatic subunits in arylphenones can effectively tune the energy level and the orbital feature of the triplet exciton. Our experimental data reveal that a series of full-color pure organic phosphors with a balanced lifetime (up to 0.23 s) and efficiency (up to 36.0%) can be realized under ambient conditions, demonstrating the validity of our instructive design principle.

INTRODUCTION

Light is emitted from luminophores and is one of the most fundamental and indispensable elements to life and society. The development of luminophores has greatly promoted high-tech innovations in energy and life sciences. For instance, luminescent materials are widely used in organic light-emitting diodes and biotechnologies. In particular, luminophores with phosphorescent emission can potentially utilize 75% of electrically generated triplet excitons[1] and function as sensitive bioimaging probes to eliminate the short-lived autofluorescence.[2] Indeed, phosphorescent materials have found wide application in electronics,[3–5] optics,[6,7] and biological areas.[8] Because the emission from the excited triplet state is sensitive to temperature and oxygen,[9] phosphorescence from a luminophore is normally observed under cryogenic and inert conditions, which has severely restricted its use in high-tech applications. Achieving materials with persistent and efficient room-temperature phosphorescence (RTP) thus has drawn extensive attention. So far, most efficient RTP luminophores are metal-containing inorganic and organometallic compounds, which generally have the drawbacks of high cost and cytotoxicity, low processability, and low flexibility and stability.[10,11] In contrast, pure organic RTP materials are attractive alternatives and have the advantages of wide variety,[12] good biocompatibility,[13] appreciable stability, and good processability.[14,15] However, developing persistent and efficient pure organic RTP materials is extremely difficult because of inefficient intersystem crossing (ISC) caused by weak spin-orbit coupling and the rapid rate of nonradiative decay.

The Bigger Picture

The development of luminophores has greatly promoted high-tech innovations in energy and life sciences. For instance, room-temperature phosphorescent (RTP) materials are attractive because of their multidisciplinary applications in electronics, optics, and biological areas. However, developing efficient and persistent RTP materials is extremely challenging for pure organic (metal-free) phosphors because of the weakness of spin-orbit coupling and the sensitivity of triplet excitons. On the one hand, tremendous efforts have been made to modulate aggregation behaviors to suppress nonradiative decay in order to achieve efficient light emission and long lifetimes. On the other hand, the molecular structure and frontier orbital can intrinsically determine their performance but have been poorly investigated. To attain such a goal, here we present a rational molecular design principle based on molecular-structure engineering to serve as a comprehensive model for the exploration of novel organic phosphors.

Recently, several groups have used different methodologies, including polymer aggregation,[16] crystallization,[17–21] halogen bonding,[22,23] self-assembly,[24,25] and H-aggregation,[26] to develop pure organic RTP systems (Figure 1). These strategies tend to modulate the aggregation behaviors of organic phosphors to suppress their nonradiative-decay pathways[27] and thus can be classified as aggregation-induced RTP (Figure 1). Several other important strategies, such as host-guest composition,[28] polymer-matrix assistance,[29,30] molecule-metal hybrids,[31] metal-organic framework hosting,[32] and so on, are also being investigated and promote the development of the area (Figure 1). Despite these exciting achievements,[33] there are few examples of organic phosphors with both high efficiency and a long lifetime.[34–36] It is also quite difficult to explore the strategies further because a comprehensive investigation on the molecular structure-property relationship is lacking.[37]

Here, we deliver a structure-property relationship from which we derive a molecular design principle on the basis of molecular-orbital investigation. This work provides rational guidelines that will undoubtedly promote the fundamental understanding and exploration of novel pure organic RTP systems from a molecular-structure perspective. Phosphors with high efficiency and long lifetimes, as well as tunable emission, were developed as a proof of concept. The experimental data reveal that balanced RTP performance can be achieved in a single luminogenic molecule.

RESULTS

Molecular-Orbital Model

The Jablonski diagram lists the typical decay pathways of the lowest singlet (S_1) and triplet (T_1) excited states (Figure 2A). For obtaining RTP materials with an efficient phosphorescence quantum yield (Φ_P) and persistent or long phosphorescence lifetime (τ_P), there are three requirements: (1) spin-flipping by an efficient ISC process from S_1 to T_n, (2) shutdown of nonradiative relaxation or a low rate of nonradiative decay (k_{ISC}') to favor phosphorescent emission from T_1 to S_0, and (3) a slow phosphorescence rate (k_P) to achieve a long τ_P (Equations 1 and 3 in Figure 2).

Phosphors with a high quantum yield of ISC (Φ_{ISC}) generally show a fast ISC rate (k_{ISC}) to compete with the rate of fluorescence decay (k_F) and the rate of internal conversion (k_{IC}) in the depopulating processes of S_1 (Equation 2 in Figure 2). The k_{ISC} can be greatly promoted by small singlet-triplet (S-T) splitting energy and effective spin-orbit coupling (SOC) between S_1 and T_n. Generally, the S-T splitting energy is large for most organic molecules without a pronounced charge-transfer character. Heavy metals such as Ir and Pt and halogen atoms can trigger significant SOC. On the other hand, for pure organic compounds, according to the El-Sayed rule,[38] effective SOC occurs in the transition from the singlet state with an electronic configuration such as $^1(n,\pi^*)$ or $^1(\pi,\pi^*)$ to a triplet state such as $^3(\pi,\pi^*)$ or $^3(n,\pi^*)$, respectively, because the orbitals can effectively overlap under the operation of the orbital angular momentum operator (Figure 2C). In contrast, ISC from $^1(\pi,\pi^*)$ to $^3(\pi,\pi^*)$ and $^1(n,\pi^*)$ to $^3(n,\pi^*)$ is not favored because the SOC is insignificant as a result of the inefficient orbital overlapping prohibited by the angular momentum operator. Thus, the existence of n orbitals that are perpendicular to the π orbitals becomes crucial for triggering striking SOC and turning on the ISC process from the singlet to the triplet state.

Persistent pure organic RTP materials require that τ_P shows in a second range and thus need a slow decay process of T_1. As mentioned, T_1 with a $^3(\pi,\pi^*)$ configuration can show an extremely slow decay rate ($\sim 10^0$ s^{-1}) because of the forbidden

[1]Department of Chemistry, Institute of Molecular Functional Materials, Hong Kong Branch of Chinese National Engineering Research Center for Tissue Restoration and Reconstruction, Hong Kong University of Science and Technology, Clear Water Bay, Kowloon, Hong Kong, China

[2]Key Laboratory of Organic Solids, Beijing National Laboratory for Molecular Science, Institute of Chemistry, Chinese Academy of Sciences, Beijing 100190, China

[3]Key Laboratory of Organic OptoElectronics and Molecular Engineering, Department of Chemistry, Tsinghua University, Beijing 100084, China

[4]Department of Applied Physics, Hong Kong Polytechnic University, Hong Kong, China

[5]Shenzhen Research Institute, Hong Kong University of Science and Technology, No. 9 Yuexing 1st Road, South Area, Hi-tech Park, Nanshan, Shenzhen 518057, China

[6]Guangdong Innovative Research Team, SCUT-HKUST Joint Research Laboratory, State Key Laboratory of Luminescent Materials and Devices, South China University of Technology, Guangzhou 510640, China

[7]Co-first author

[8]Lead Contact

*Correspondence: qpeng@iccas.ac.cn (Q.P.), tangbenz@ust.hk (B.Z.T.)

http://dx.doi.org/10.1016/j.chempr.2016.08.010

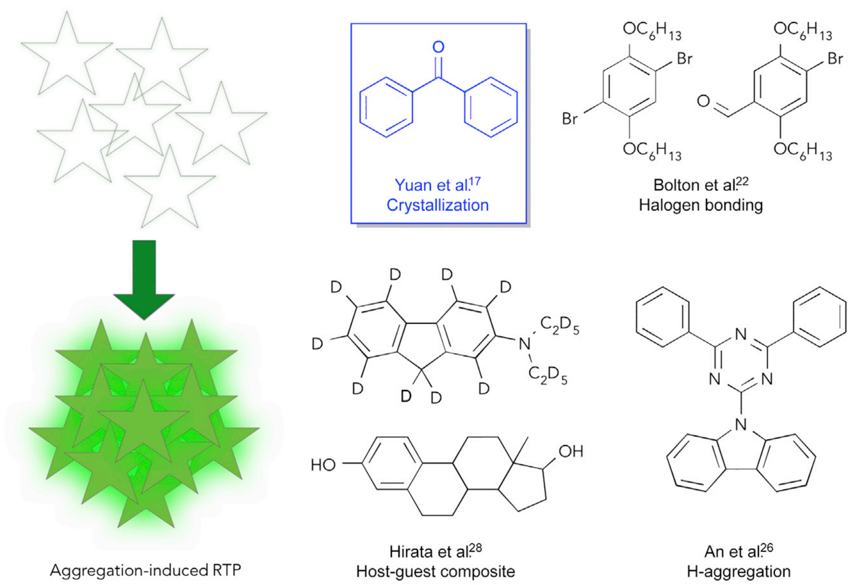

Figure 1. Strategies for Developing Pure Organic RTP Systems
Schematic representations of modulating the aggregation behaviors of organic phosphors to suppress nonradiative-decay pathways and achieve RTP. These strategies are classified as aggregation-induced RTP. Selected representative examples of pure organic RTP materials developed by different methodologies are shown.

transition from $^3(\pi,\pi^*)$ to $^1\pi^2$.[39] Endowing phosphors with an electronic configuration of $^3(\pi,\pi^*)$ is therefore key to obtaining a long-lived T_1. However, in pure organic compounds, T_1 is rarely either pure $^3(\pi,\pi^*)$ or $^3(n,\pi^*)$ but is rather a hybrid mixture of the two configurations with different proportions of $\alpha_n{}^3(n,\pi^*) + \beta_\pi{}^3(\pi,\pi^*)$, where $\alpha_n + \beta_\pi = 1$ (Figure 2C). The T_1 state with a hybrid configuration gives a moderate but tunable k_P. Thus, the molecular design of the excited state with hybrid (n,π^*) and (π,π^*) configurations in appreciable proportion is desired for obtaining efficient persistent RTP materials.

From the above discussion, (1) the existence of n orbitals and (2) the T_1 state with a nearly pure $^3(\pi,\pi^*)$ configuration are the general structural requirements for developing a pure organic persistent and efficient RTP phosphor without heavy atoms. Following such a molecular design rule, we first chose carbonyl groups (C=O) to provide n orbitals to trigger the ISC from S_1 to T_n. Then, we incorporated various conjugated subunits to introduce π orbitals and reduce k_P. Last, five pure organic molecules with molecular structures as shown in Figure 3 were designed and synthesized. Detailed procedures for their synthesis and characterization are given in the Supplemental Information. As expected, the carbonyl groups selected from various heteroatomic groups have n orbitals, which provide effective SOC-induced ISC of S_1 to T_n and hence high Φ_{ISC}. Importantly, with the π-extended subunits, the T_1 state has a high character of $^3(\pi,\pi^*)$ configuration, resulting in a persistent lifetime. The variation of aryl groups mixes the pure (n,π^*) and (π,π^*) molecular orbitals, giving tunable T_1 states with different energy levels and a $^3(\pi,\pi^*)$ character, which in turn affects the phosphorescence color, efficiency, and lifetime. Furthermore, in the crystal state, the vibrational motions are largely suppressed to block the nonradiative decay of T_1 as a result of the environmental constraint.[17,20,27] Thus, we chose crystallization here as an effective rigidification tool to trigger the RTP by blocking oxygen quenching and other nonradiative-decay pathways. As a result, remarkably

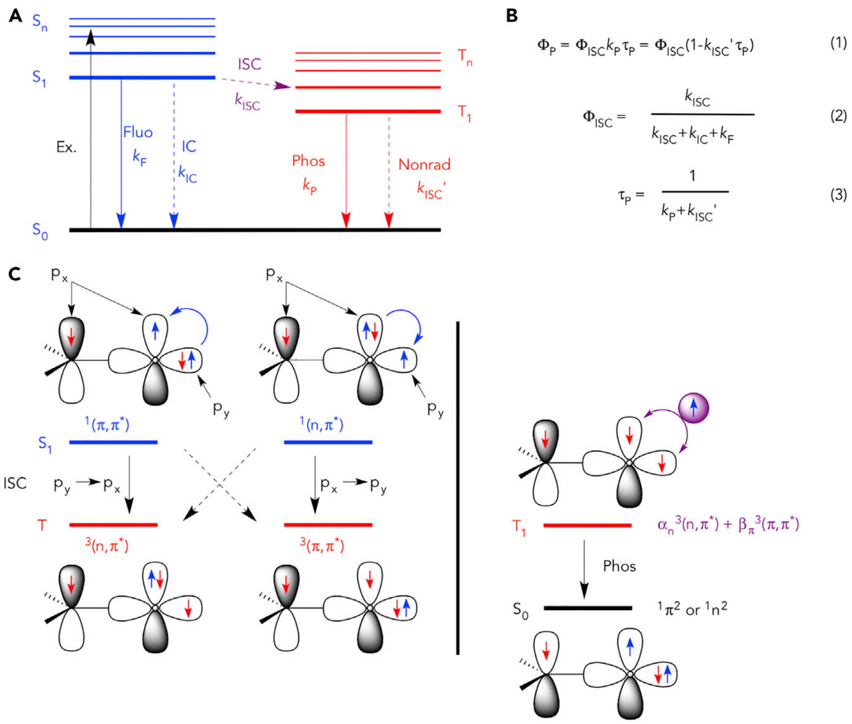

Figure 2. Theoretical Models for Understanding the Performance of Pure Organic RTP

(A) A Jablonski diagram of organic luminophores.

(B) Equations for phosphorescence quantum yield, ISC quantum yield, and phosphorescence lifetime.

(C) Schematic representation of the El-Sayed rule for ISC and molecular-orbital hybridization of the lowest triplet states for tuning the rate of phosphorescence decay. Generally, persistent organic phosphorescence results from an extremely slow radiative decay rate of T_1 with a pure $^3(\pi,\pi^*)$ configuration.

fast k_{ISC}, tunable k_P, and slow k_{ISC}' can be realized in our system. The Φ_P of the pure organic molecules prepared can reach 34.5% with a long second-order lifetime.

Theoretical Calculations

To validate our assumption and gain more insight into the mechanism of RTP, we performed first-principle density functional theory (DFT) and time-dependent DFT (TD-DFT) calculations on molecules **1**–**5**. For comparison, benzophenone (BP, **6**), benzil (**7**), and difluorobenzophenone (DFBP, **8**), whose molecular structures are shown in the Supplemental Information, were also included in the analysis (see section "Theoretical and Computational Methods" in Supplemental Information, Figures S10–S14, and Tables S3–S5). The calculated energy gap (ΔE_{S1Tn}), the SOC constant between S_1 and the involved triplet state (ξ_{S1Tn}), and the proportions of $^3(n,\pi^*)$ (α_n) and $^3(\pi,\pi^*)$ (β_π) configurations in the S_1 and T_n states for 1-(dibenzo[*b*,*d*]furan-2-yl)phenylmethanone (BDBF, **3**) are given in the inset of Figure 4A; the values for other compounds are provided in Figure S1. From the data, the relationships between ξ_{S1Tn} and $\Delta\alpha_n$ ($=|\alpha_{n,S1}-\alpha_{n,Tn}|$) and τ_P and β_π in the T_1 state for **1**–**8** were established. The calculated energy gaps between S_1 and T_1 were considerably large for **1**–**8** (>0.6 eV), which blocks the reversible ISC from T_1 to S_1 for thermally activated delayed fluorescence and weakens the phosphorescence.[40,41]

It is easily seen that the extent of SOC, and hence the efficiency of the ISC process from S_1 to T_n, is really actuated by the characters of the excited states. As shown in

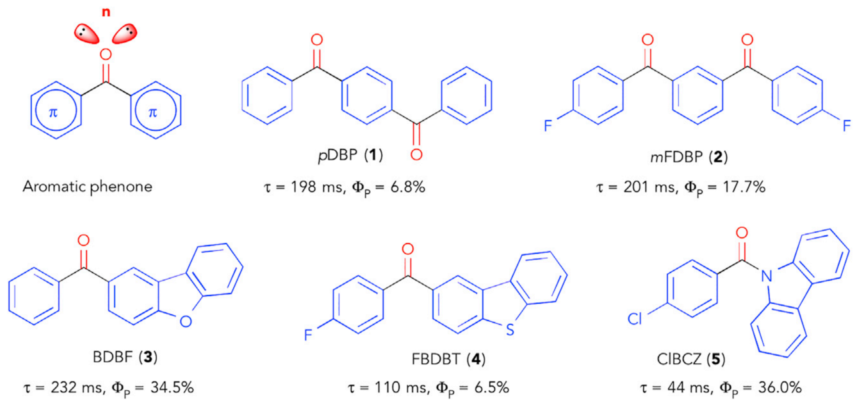

Figure 3. Structures of Organic Molecules Studied in This Work with Tunable RTP Lifetimes and Efficiencies

The incorporation of carbonyl groups with non-bonding electrons aims to promote efficient ISC. The different aromatic substituents are introduced to support the formation of $^3(\pi,\pi^*)$ as the lowest excited triplet state T_1 with different energy levels and amounts of mixing with n orbitals.

Figure 4A, when the $\Delta\alpha_n$ value became larger, stronger coupling was observed because it promoted $n \leftrightarrow \pi$ or single-center $p_x \rightarrow p_y$ transition. On the other hand, as described above, the ISC process was also facilitated by a small energy gap (ΔE_{ST}) between the two states. This explains why (9H-carbazol-9-yl)(4-chlorophenyl)methadone (ClBCZ, **5**) (not given in Figure 4) showed a low $\Delta\alpha_n$ value but still exhibited quite an efficient ISC process as a result of the narrow energy gap (ΔE_{S1T3} = 0.02 eV) between S_1 and T_3. Analysis of the proportions of the $^3(n,\pi^*)$ (α_n) and $^3(\pi,\pi^*)$ (β_π) configurations at the T_1 state elucidated the features of the excited states. As depicted in Figure 4B, molecules **6–8** showed a β_π value lower than 50%. Thus, excited states with a predominant $^3(n,\pi^*)$ configuration were realized. On the other hand, molecules **1–3** possessed large aromatic subunits. This endowed their excited states with higher $^3(\pi,\pi^*)$ characteristics and hence high β_π values above 70%. Generally, molecules with a major $^3(n,\pi^*)$ configuration show a faster k_P and hence a shorter τ_P than those with a $^3(\pi,\pi^*)$ configuration because of the availability of the spin-flip process and $n \leftrightarrow \pi$ or $p_x \rightarrow p_y$ transition. Compound **3** or BDBF, for example, possessed a typical $^1(n,\pi^*)$ S_1 state, a low-lying hybrid $^3(n,\pi^*)$ and $^3(\pi,\pi^*)$ T_2 state, and a typical $^3(\pi,\pi^*)$ T_1 state. The relatively smaller energy gap and larger $\Delta\alpha_n$ value from S_1 to T_2 made the $S_1 \rightarrow T_2$ transition the key channel to populate the triplet state. The large value of β_π in T_1 suggests its high $^3(\pi,\pi^*)$ feature and hence its slow k_P and long τ_P.

Experimental Investigation

Benzophenone (**6**) is an archetypal phosphor and exhibits short-lived (~milliseconds) phosphorescence both in solution at low temperature[42] and in the crystalline state at room temperature.[17] Incorporating different π-extended groups such as benzoyl, benzofuranyl, benzothiophenyl, and carbazolyl groups into its structure afforded five luminophores, namely 1,4-phenylene bis(phenylmethanone) (*p*DBP, **1**), 1,3-phenylene bis(4-fluorophenyl)methadone (*m*FDBP, **2**), BDBF (**3**), dibenzo[b,d]thiophen-2-yl(4-fluorophenyl)methadone (FBDBT, **4**), and ClBCZ (**5**). Their photophysical properties were systematically investigated in different states. These molecules were found to be non-luminescent in the solution and amorphous states but strongly emissive in the crystalline phase in ambient conditions. This suggests that crystallization induced RTP in these molecules, which is commonly observed in luminogens with aggregation-induced emission characteristics.[43]

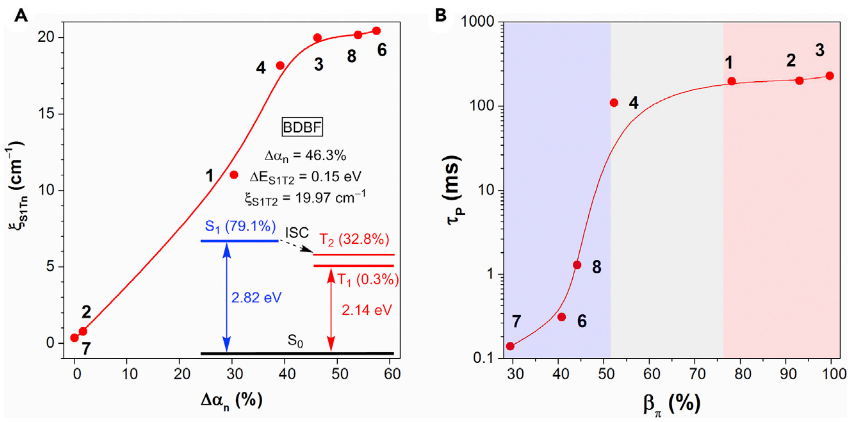

Figure 4. Theoretical Calculations for Mechanistic Investigation

(A) Relationship between the spin-orbit coupling constant (ξ_{S1Tn}) and the change in the proportion of the $^3(n,\pi^*)$ configuration ($\Delta\alpha_n$) during the transition from S_1 to T_n by TD-DFT calculations. Inset: diagrams of the calculated energy levels, main orbital configurations at the singlet (S_1) and triplet (T_n) states, and ξ_{S1Tn} of BDBF (values of α_n are given in parentheses).

(B) Plot of the experimental phosphorescence lifetime (τ_P) against the proportion of the $^3(\pi,\pi^*)$ configuration (β_π) at the T_1 state.

As a proof of concept, we describe BDBF as a representative for discussion. As suggested by the powder X-ray diffraction (PXRD) shown in Figure S2A, the BDBF powder obtained by two rounds of recrystallization from dichloromethane and hexane was crystalline, whereas the one obtained by heating the powder with a heating gun and then quenching the melt with liquid nitrogen was amorphous. Analysis of the time-resolved excitation and emission spectra given in Figures S2B and S2C revealed that the best excitation and emission wavelengths for BDBF for achieving efficient and persistent RTP are 350–400 and 550 nm, respectively.

Thus, when the crystalline BDBF powder was irradiated with 365 nm UV light at 300 and 77 K in air, intense green emission was observed. In contrast, its solution and amorphous powder emitted only at 77 K (Figure 5A). The steady-state photoluminescence (PL) spectra of the crystalline powder measured in air and in an inert atmosphere were almost identical, revealing that crystallization is an effective rigidification tool for triggering RTP by blocking emission quenching by oxygen and other nonradiative-decay pathways (Figure S2B). On the other hand, the phosphorescence feature of BDBF was intrinsic because of the large similarity between the PL spectrum and lifetime-decay curve at different states at 77 K (Figure 5B). In another experiment, we investigated the temperature effect on the PL of BDBF. With an increase in the temperature from 50 to 350 K, the emission of BDBF became weaker, probably because excited states have a higher probability of relaxing through nonradiative channels at elevated temperatures (Figure 5C). The time-resolved PL-decay curves of the crystalline powder measured at different wavelengths at 50 K demonstrate the pure phosphorescence characteristics of the luminescence. The photographs taken of the crystalline, solution, and amorphous samples in the presence and absence of the excitation source at 77 K and their associated spectra of prompt and delayed PL also suggest a similar idea (Figure S3). After removal of the excitation source, the emission faded slowly and could be followed by the naked eye (Figure 3D inset). The measured and calculated luminescence lifetimes at 300 K were the same and equal to 0.23 s, which is quite long among the reported RTP systems. The emission was strong with a Φ_P of 34.5% in ambient conditions. On careful examination of the PL spectra and decay curves, we found the presence of two

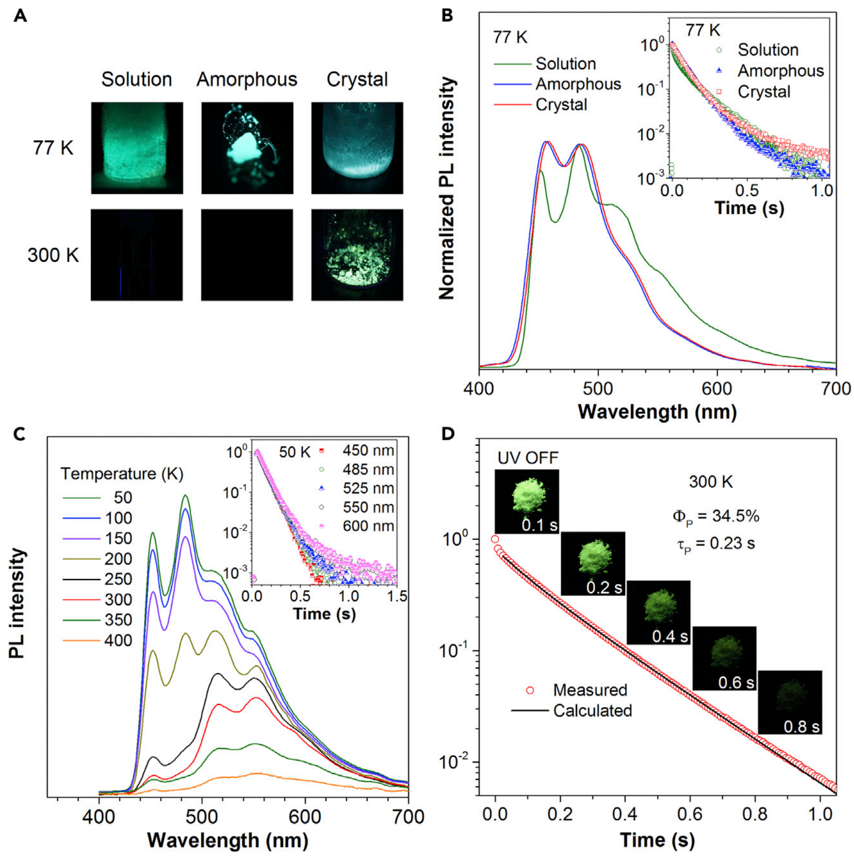

Figure 5. Photophysical Properties of BDBF

(A) Photographs of BDBF solution (10^{-4} M in cyclohexane), amorphous powder, and crystalline powder under 365 nm UV irradiation at 77 K and 300 K.

(B) PL spectra of BDBF solution, amorphous powder, and crystalline powder at 77 K. Inset: time-resolved PL-decay curves of BDBF solution, amorphous powder, and crystalline powder at 525 nm and 77 K.

(C) PL spectra of BDBF measured at different temperatures from 50 to 400 K. Inset: time-resolved PL-decay curves of BDBF at 450, 485, 525, 550, and 600 nm and 50 K indicate the pure phosphorescence feature of the emission.

(D) Time-resolved PL-decay curve of BDBF at 300 K. Inset: photographs of the time-dependent emission decay of BDBF crystalline powder under 365 nm UV irradiation.

emitting species with different overlapping emission spectra and lifetimes. As a result, the spectra of prompt and delayed PL at 77 K were similar but not exactly the same; they showed slightly difference peaks, and the spectrum of delayed PL included a tail (Figures 5B and S3). On further analysis of the decay curves, two-component (exponential) decays were seen to coexist in each emission band (Figure 5C, inset, and Table S1). Emission at shorter wavelengths consisted of faster decay and was quite sensitive to temperature. With decreasing temperature, emission at shorter wavelengths was greatly enhanced and became the dominant profile.

Similarly, the crystalline and amorphous samples of *p*DBP (**1**), *m*FDBP (**2**), FBDBT (**4**), and ClBCZ (**5**) were prepared and analyzed by PXRD (Figure S4). Similar to BDBF, these molecules exhibited bright phosphorescence in solutions (Figure S5) and amorphous states (Figure S6) at 77 K and stronger emission in the crystalline states (Figure S7) at low temperatures. As mentioned above, the π-extended units exerted a strong influence on the electronic properties or the emission behaviors of the

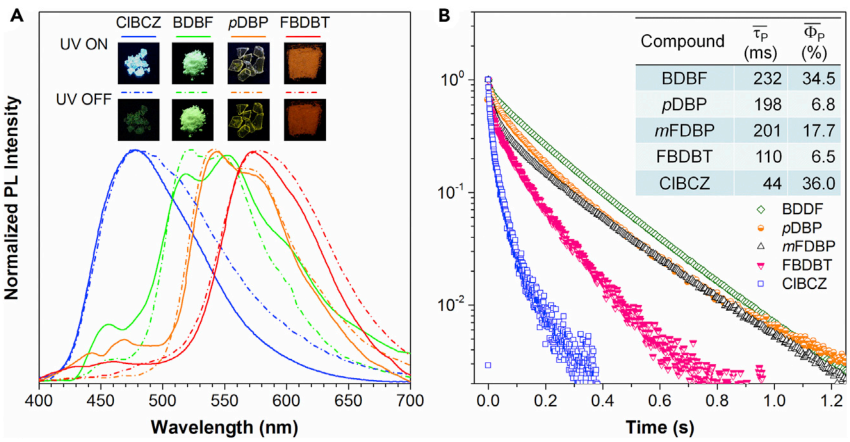

Figure 6. Versatile RTP Molecules with Tunable Colors and Lifetimes under Ambient Conditions
(A) The steady-state spectra of prompt (solid line) and delayed (dashed line, 10 ms) phosphorescence. Insets show the corresponding photographs taken before (up) and after (down) the excitation source was turned off. The compounds were excited at 365 nm at their crystalline states.
(B) Time-resolved PL-decay curves of BDBF, *p*DBP, *m*FDBP, FBDBT, and ClBCZ. The inset shows their average lifetimes and phosphorescence quantum yields.

luminogens. As shown in Figure 6A, changing the aryl group varied the energy gap between T_1 and S_0, which changed the emission color of the molecules from blue to green to yellow, and even to orange-red. The lifetimes of most of the molecules were in hundreds of milliseconds, demonstrating the persistent nature of their emission (Figure 6B). In brief, *p*DBP (**1**) crystals emitted yellow light with a Φ_P of 6.8%, and the crystalline powders of *m*FBDBF (**2**) showed a more intense green light with a higher Φ_P of 17.7%. On the other hand, FBDBT (**4**) crystals emitted pink light with a low Φ_P of 6.5%, but ClBCZ (**5**) crystals emitted an intense green light with the highest quantum yield of 36.0% and a shorter lifetime of 44 ms. The detailed lifetimes, quantum yields, and decay constants are summarized in Table S2. The nanosecond decay curves of the molecules and benzophenone are shown in Figure S8. No emission decay was detected in the nanosecond range, and all spectra coincided well with the spectrum in the absence of sample, demonstrating that the molecules synthesized in the present study are pure phosphors.

DISCUSSION

As revealed by our experimental data, we successfully achieved phosphors with tunable emission colors (from blue to orange-red), high efficiencies (up to 36.0%), and persistent lifetimes (up to 0.23 s) by using a proper π-conjugated system. Furthermore, we achieved persistent and efficient RTP achieved in a single molecule such as BDBF under ambient conditions. Although the performance was impressive, both the lifetime and efficiency were still lower than the best previously reported values. Careful examination of the performance of previous systems reveals a conflict. Generally, systems showing high efficiencies have short lifetimes in microseconds,[22,23] whereas those with persistent lifetimes have low phosphorescence efficiencies.[26,28] According to Equation 1, $\Phi_P = \Phi_{ISC}(1-k_{ISC}'\tau_P)$ shown in Figure 2B, using the same rigidification methodology suppresses k_{ISC}' to almost the same level. Obviously, the increase in lifetime will simultaneously decrease the efficiency. On the one hand, a slow k_P (e.g., 10^{-3} s^{-1} in Huang's H-aggregation system[26]) is needed for achieving a persistent lifetime but cannot easily compete with k_{ISC}' and will thus have a low efficiency. On the other hand, a high k_P will lead to a short lifetime but high efficiency as a result of the better competition with k_{ISC}' (e.g., Kim's halogen bonding system[22,23]). As a result, endowing a persistent RTP system with high efficiency becomes more difficult than for systems with short lifetimes. If we can suppress k_{ISC}' to an ignorable level (~0 s^{-1}), which is impossible, we could obtain RTP systems with both high efficiency and a persistent lifetime. However, this possibility is extremely challenging under ambient conditions. As a proof of concept, here we present a system with balanced performance in terms of efficiency and lifetime.

Figure 4B demonstrates the correlation between β_π and the measured τ_P and calculated k_P. The large dependence of τ_P on β_π reveals that the molecular-orbital feature of T_1 determines the k_P. A high β_π suggests a nearly pure $^3(\pi,\pi^*)$ characteristic of T_1, which shows a slow k_P and relaxes through a persistent phosphorescence-decay pathway. Importantly, the experimental results validate the molecular-orbital model and theoretical calculations, which can serve as an attractive endeavor for elucidating the fundamental structure-property relationship.

In summary, we present a clear picture for comprehensive understanding of the phosphorescence process of pure organic materials. The principle, which involves adjusting the characteristics of molecular orbitals and the exciton configuration in the excited state by varying the molecular structure, provides a tool for modulating the intrinsic RTP performance. Theoretical investigations on molecular orbitals reveal that the electronic configuration of the exciton is crucial to ISC and the decay of radiative phosphorescence. Thus, the molecular design of an excited state with hybrid configurations (n,π^*) and (π,π^*) in appreciable proportion is desired for obtaining efficient persistent RTP materials. By tuning the features of the molecular orbital and the energy level of the excited state through tailoring the aromatic subunits in arylphenones, we obtained a series of full-color pure organic phosphors with an efficiency of up to 36.0% and a long lifetime of 0.23 s under ambient conditions. The key issue is the synergistic effect of aromatic subunits and ketones, which realizes remarkably fast k_{ISC} and slow k_P to afford balanced performance. The rational guidelines gained from our experimental and theoretical investigations will allow for the exploration of novel organic phosphors.

EXPERIMENTAL PROCEDURES

All chemicals and other reagents were purchased from Aldrich and used as received without further purification. All molecules synthesized were purified by column chromatography, recrystallized twice from dichloromethane and hexane, and fully characterized by ^{1}H nuclear magnetic resonance (NMR), ^{13}C NMR, high-resolution mass spectroscopy, and elemental analysis. The photoluminescence spectra were measured on a PerkinElmer LS 55 spectrophotometer. The lifetime, time-resolved excitation spectra, steady-state and time-resolved emission spectra, temperature-dependent photoluminescence spectra, and absolute luminescence quantum yield were measured on an Edinburgh FLSP920 fluorescence spectrophotometer equipped with a xenon arc lamp (Xe900), a microsecond flash lamp (uF900), a picosecond pulsed diode laser (EPL-375), a closed-cycle cryostate (CS202*I-DMX-1SS, Advanced Research Systems), and an integrating sphere (0.1 nm step size, 0.3 s integration time, five repeats), respectively. Mean decay times (τ_P) were obtained from individual lifetimes (τ_i) and amplitudes (a_i) of multi-exponential evaluations. PXRD patterns were performed on an X'Pert PRO MPD diffractometer with Cu Kα radiation (λ = 1.5418 Å) at 25°C (scan range: 4.5°–50°). Single-crystal data were collected on a Bruker Smart APEXII CCD diffractometer using graphite-monochromated Cu Kα radiation (λ = 1.54178 Å). Photos were recorded with a Cannon EOS 60D. The DFT and TD-DFT calculations were performed with a Gaussian 09 program.

SUPPLEMENTAL INFORMATION

Supplemental Information includes Supplemental Experimental Procedures, 14 figures, and 5 tables and can be found with this article online at http://dx.doi.org/10.1016/j.chempr.2016.08.010.

AUTHOR CONTRIBUTIONS

W.Z. synthesized all materials and performed all photophysical measurements. Z.H. and W.Z. grew the crystals, analyzed the data, and prepared the paper. W.Z. and Z.H. contributed equally to this work. H.M., Z.S., and Q.P. performed the theoretical calculations. G.B. and J.H. assisted with measuring photophysical properties. J.W.Y.L. and B.Z.T. designed and supervised the research and wrote the paper. All authors discussed the results and commented on the manuscript.

ACKNOWLEDGMENTS

The authors acknowledge financial support from the National Basic Research Program of China 973 Program (2013CB834701), the Research Grants Council of Hong Kong (16301614, 16305015, and N_HKUST604/14), the University Grants Committee of Hong Kong (AoE/P-03/08), and the Innovation and Technology Commission (ITC-CNERC14SC01). Q.P. thanks the National Natural Science Foundation of China (1473214, 21503118, and 21290191). B.Z.T. thanks the Guangdong Innovative Research Team Program (201101C0105067115) for financial support.

Received: July 14, 2016
Revised: August 11, 2016
Accepted: August 18, 2016
Published: October 13, 2016

REFERENCES AND NOTES

1. Pope, M., Kallmann, H.P., and Magnante, P. (1963). Electroluminescence in organic crystals. J. Chem. Phys. *38*, 2042–2043.
2. Maldiney, T., Lecointre, A., Viana, B., Bessière, A., Bessodes, M., Gourier, D., Richard, C., and Scherman, D. (2011). Controlling electron trap depth to enhance optical properties of persistent luminescence nanoparticles for in vivo imaging. J. Am. Chem. Soc. *133*, 11810–11815.
3. Shao, Y., and Yang, Y. (2005). Efficient organic heterojunction photovoltaic cells based on triplet materials. Adv. Mater. *17*, 2841–2844.
4. Baldo, M.A., O'Brien, D.F., You, Y., Shoustikov, A., Sibley, S., Thompson, M.E., and Forrest, S.R. (1998). Highly efficient phosphorescent emission from organic electroluminescent devices. Nature *395*, 151–154.
5. Kabe, R., Notsuka, N., Yoshida, K., and Adachi, C. (2016). Afterglow organic light-emitting diode. Adv. Mater. *28*, 655–660.
6. Hirata, S., Totani, K., Yamashita, T., Adachi, C., and Vacha, M. (2014). Large reverse saturable absorption under weak continuous incoherent light. Nat. Mater. *13*, 938–946.
7. Sun, H., Liu, S., Lin, W., Zhang, K.Y., Lv, W., Huang, X., Huo, F., Yang, H., Jenkins, G., Zhao, Q., et al. (2014). Smart responsive phosphorescent materials for data recording and security protection. Nat. Commun. *5*, 3601.
8. Zhang, G., Palmer, G.M., Dewhirst, M.W., and Fraser, C.L. (2009). A dual-emissive-materials design concept enables tumour hypoxia imaging. Nat. Mater. *8*, 747–751.
9. Menning, S., Kramer, M., Coombs, B.A., Rominger, F., Beeby, A., Dreuw, A., and Bunz, U.H. (2013). Twisted tethered tolanes: unanticipated long-lived phosphorescence at 77 K. J. Am. Chem. Soc. *135*, 2160–2163.
10. Zhang, Y., Lee, J., and Forrest, S.R. (2014). Tenfold increase in the lifetime of blue phosphorescent organic light-emitting diodes. Nat. Commun. *5*, 5008.
11. Lee, J., Chen, H.-F., Batagoda, T., Coburn, C., Djurovich, P.I., Thompson, M.E., and Forrest, S.R. (2015). Deep blue phosphorescent organic light-emitting diodes with very high brightness and efficiency. Nat. Mater. *15*, 92–98.
12. Yoshii, R., Hirose, A., Tanaka, K., and Chujo, Y. (2014). Functionalization of boron diiminates with unique optical properties: multicolor tuning of crystallization-induced emission and introduction into the main chain of conjugated polymers. J. Am. Chem. Soc. *136*, 18131–18139.
13. Zheng, X., Wang, X., Mao, H., Wu, W., Liu, B., and Jiang, X. (2015). Hypoxia-specific ultrasensitive detection of tumours and cancer cells in vivo. Nat. Commun. *6*, 5834.
14. Lee, D., Bolton, O., Kim, B.C., Youk, J.H., Takayama, S., and Kim, J. (2013). Room temperature phosphorescence of metal-free organic materials in amorphous polymer matrices. J. Am. Chem. Soc. *135*, 6325–6329.
15. Kwon, M.S., Lee, D., Seo, S., Jung, J., and Kim, J. (2014). Tailoring intermolecular interactions for efficient room-temperature phosphorescence from purely organic materials in amorphous polymer matrices. Angew. Chem. Int. Ed. Engl. *53*, 11177–11181.
16. Zhang, G., Chen, J., Payne, S.J., Kooi, S.E., Demas, J.N., and Fraser, C.L. (2007). Multi-emissive difluoroboron dibenzoylmethane polylactide exhibiting intense fluorescence and oxygen-sensitive room-temperature phosphorescence. J. Am. Chem. Soc. *129*, 8942–8943.
17. Yuan, W.Z., Shen, X.Y., Zhao, H., Lam, J.W.Y., Tang, L., Lu, P., Wang, C., Liu, Y., Wang, Z., Zheng, Q., et al. (2010). Crystallization-induced

phosphorescence of pure organic luminogens at room temperature. J. Phys. Chem. C *114*, 6090–6099.

18. Bergamini, G., Fermi, A., Botta, C., Giovanella, U., Di Motta, S., Negri, F., Peresutti, R., Gingras, M., and Ceroni, P. (2013). A persulfurated benzene molecule exhibits outstanding phosphorescence in rigid environments: from computational study to organic nanocrystals and OLED applications. J. Mater. Chem. C *1*, 2717–2724.

19. Fermi, A., Bergamini, G., Peresutti, R., Marchi, E., Roy, M., Ceroni, P., and Gingras, M. (2014). Molecular asterisks with a persulfurated benzene core are among the strongest organic phosphorescent emitters in the solid state. Dyes Pigm. *110*, 113–122.

20. Gong, Y., Zhao, L., Peng, Q., Fan, D., Yuan, W.Z., Zhang, Y., and Tang, B.Z. (2015b). Crystallization-induced dual emission from metal- and heavy atom-free aromatic acids and esters. Chem. Sci. *6*, 4438–4444.

21. Li, C., Tang, X., Zhang, L., Li, C., Liu, Z., Bo, Z., Dong, Y.Q., Tian, Y.-H., Dong, Y., and Tang, B.Z. (2015). Reversible luminescence switching of an organic solid: controllable on–off persistent room temperature phosphorescence and stimulated multiple fluorescence conversion. Adv. Opt. Mater. *3*, 1184–1190.

22. Bolton, O., Lee, K., Kim, H.J., Lin, K.Y., and Kim, J. (2011). Activating efficient phosphorescence from purely organic materials by crystal design. Nat. Chem. *3*, 205–210.

23. Bolton, O., Lee, D., Jung, J., and Kim, J. (2014). Tuning the photophysical properties of metal-free room temperature organic phosphors via compositional variations in bromobenzaldehyde/dibromobenzene mixed crystals. Chem. Mater. *26*, 6644–6649.

24. Fermi, A., Bergamini, G., Roy, M., Gingras, M., and Ceroni, P. (2014). Turn-on phosphorescence by metal coordination to a multivalent terpyridine ligand: a new paradigm for luminescent sensors. J. Am. Chem. Soc. *136*, 6395–6400.

25. Wang, H., Wang, H., Yang, X., Wang, Q., and Yang, Y. (2015). Ion-unquenchable and thermally "on–off" reversible room temperature phosphorescence of 3-bromoquinoline induced by supramolecular gels. Langmuir *31*, 486–491.

26. An, Z., Zheng, C., Tao, Y., Chen, R., Shi, H., Chen, T., Wang, Z., Li, H., Deng, R., Liu, X., et al. (2015). Stabilizing triplet excited states for ultralong organic phosphorescence. Nat. Mater. *14*, 685–690.

27. Gong, Y., Chen, G., Peng, Q., Yuan, W.Z., Xie, Y., Li, S., Zhang, Y., and Tang, B.Z. (2015a). Achieving persistent room temperature phosphorescence and remarkable mechanochromism from pure organic luminogens. Adv. Mater. *27*, 6195–6201.

28. Hirata, S., Totani, K., Zhang, J., Yamashita, T., Kaji, H., Marder, S.R., Watanabe, T., and Adachi, C. (2013). Efficient persistent room temperature phosphorescence in organic amorphous materials under ambient conditions. Adv. Funct. Mater. *23*, 3386–3397.

29. Kwon, M.S., Yu, Y., Coburn, C., Phillips, A.W., Chung, K., Shanker, A., Jung, J., Kim, G., Pipe, K., Forrest, S.R., et al. (2015). Suppressing molecular motions for enhanced room-temperature phosphorescence of metal-free organic materials. Nat. Commun. *6*, 8947.

30. Chen, X., Xu, C., Wang, T., Zhou, C., Du, J., Wang, Z., Xu, H., Xie, T., Bi, G., Jiang, J., et al. (2016). Versatile room-temperature-phosphorescent materials prepared from N-substituted naphthalimides: emission enhancement and chemical conjugation. Angew. Chem. Int. Ed. Engl. *55*, 9872–9876.

31. Yang, X., and Yan, D. (2016). Strongly enhanced long-lived persistent room temperature phosphorescence based on the formation of metal–organic hybrids. Adv. Opt. Mater. *4*, 897–905.

32. Mieno, H., Kabe, R., Notsuka, N., Allendorf, M.D., and Adachi, C. (2016). Long-lived room-temperature phosphorescence of coronene in zeolitic imidazolate framework ZIF-8. Adv. Opt. Mater. *4*, 1015–1021.

33. Mukherjee, S., and Thilagar, P. (2015). Recent advances in purely organic phosphorescent materials. Chem. Commun. *51*, 10988–11003.

34. Yang, Z., Mao, Z., Zhang, X., Ou, D., Mu, Y., Zhang, Y., Zhao, C., Liu, S., Chi, Z., Xu, J., et al. (2016). Intermolecular electronic coupling of organic units for efficient persistent room-temperature phosphorescence. Angew. Chem. Int. Ed. Engl. *55*, 2181–2185.

35. Shimizu, M., Kimura, A., and Sakaguchi, H. (2016). Room-temperature phosphorescence of crystalline 1,4-bis(aroyl)-2,5-dibromobenzenes. Eur. J. Org. Chem. *2016*, 467–473.

36. Shimizu, M., Shigitani, R., Nakatani, M., Kuwabara, K., Miyake, Y., Tajima, K., Sakai, H., and Hasobe, T. (2016). Siloxy group-induced highly efficient room temperature phosphorescence with long lifetime. J. Phys. Chem. C *120*, 11631–11639.

37. Ward, J.S., Nobuyasu, R.S., Batsanov, A.S., Data, P., Monkman, A.P., Dias, F.B., and Bryce, M.R. (2016). The interplay of thermally activated delayed fluorescence (TADF) and room temperature organic phosphorescence in sterically-constrained donor-acceptor charge-transfer molecules. Chem. Commun. *52*, 2612–2615.

38. Lower, S.K., and El-Sayed, M.A. (1966). The triplet state and molecular electronic processes in organic molecules. Chem. Rev. *66*, 199–241.

39. Turro, N.J., Scaiano, J.C., and Ramamurthy, V., eds. (2010). Modern Molecular Photochemistry of Organic Molecules (University Science Books).

40. Uoyama, H., Goushi, K., Shizu, K., Nomura, H., and Adachi, C. (2012). Highly efficient organic light-emitting diodes from delayed fluorescence. Nature *492*, 234–238.

41. Goushi, K., Yoshida, K., Sato, K., and Adachi, C. (2012). Organic light-emitting diodes employing efficient reverse intersystem crossing for triplet-to-singlet state conversion. Nat. Photon. *6*, 253–258.

42. Kearns, D.R., and Case, W.A. (1966). Investigation of singlet → triplet transitions by the phosphorescence excitation method. III. aromatic ketones and aldehydes. J. Am. Chem. Soc. *88*, 5087–5097.

43. Mei, J., Leung, N.L.C., Kwok, R.T.K., Lam, J.W.Y., and Tang, B.Z. (2015). Aggregation-induced emission: together we shine, united we soar! Chem. Rev. *115*, 11718–11940.